Q of the Earth

DON L. ANDERSON AND R. S. HART

Seismological Laboratory, Division of Geological and Planetary Sciences
California Institute of Technology, Pasadena, California 91125

Regional body wave and surface wave studies indicate that there is a low-Q upper mantle layer underlying a high-Q lithosphere. Great circle surface wave attentuation is used to refine the Q structure of the upper mantle and to demonstrate that these features are consistent with the global data. Body wave results are used to constrain the average Q of various regions of the mantle and core and the Q gradient in the lower mantle. Normal mode data are used to test the hypotheses that bulk dissipation is not required in the mantle and that the inner core has low Q. Both hypotheses are consistent with the data. The data are also consistent with a smooth increase of Q with depth over most of the lower mantle and a low-Q zone at the base of the mantle. The radial modes require bulk dissipation somewhere in the earth, probably in the inner core. A series of parametric models is presented which illustrate the sensitivity of the attentuation data to major features of the Q distribution.

INTRODUCTION

There have been many recent studies of the elastic structure of the earth's interior, and the available data have been fit to high precision [e.g., *Dziewonski and Gilbert*, 1972; *Jordan and Anderson*, 1974; *Gilbert and Dziewonski*, 1975; *Anderson and Hart*, 1976]. The effect of anelasticity has been shown to be important [*Jeffreys*, 1965; *Liu et al.*, 1976; *Randall*, 1976; *Anderson et al.*, 1976; *Kanamori and Anderson*, 1977], and earth models have been derived which satisfy both the free oscillation and the body wave data [*Akopyan et al.*, 1975; *Anderson and Hart*, 1976; *Hart et al.*, 1976, 1977]. In particular, the 'base line' discrepancy for S travel times has been resolved with these later models.

The coupling between the elastic and anelastic properties of the earth and the necessity for making frequency dependent corrections to travel times and eigenperiods make it desirable to improve estimates of Q in the earth. *Anderson and Archambeau* [1964] and *Anderson et al.* [1965] investigated a range of simple Q models and concluded that there was a low-Q zone at the top of the mantle, that Q increased with depth in the mantle, and that losses in pure compression were negligible compared to those in shear. The Q model MM8, resulting from these studies, is a reasonable fit to much of the fundamental normal mode data. It does not, however, satisfy the low-order ${}_0S_l$ ($l < 10$) spheroidal modes and many of the overtones, and it was not specifically tested against the body wave or radial mode data. *Gilbert and Dziewonski* [1975] also derived a simple Q model which they used for help in identifying normal mode peaks.

We have attempted to improve upon model MM8 and to construct Q models which are compatible with both the normal mode data set, including overtones, and with teleseismic body wave observations. Although there are observational and theoretical reasons for believing that Q might not be independent of frequency, we have attempted to find such models that are consistent with as much data as possible.

The data are not yet adequate for a complete formal inversion with estimates of resolution particularly because of the unknown frequency dependence of Q and the internal inconsistencies of the available data. Our goal is rather to construct models based on body wave data and to test and modify these models by successive approximation in order to satisfy the normal mode data. In doing so we are testing the hypothesis that an earth model can be found which satisfies both body wave and normal mode attenuation observations. This is the first step in a program that will ultimately include frequency dependence. We will show that most of the available attenuation data are consistent with frequency independent Q versus depth models. Frequency dependent Q models are treated later.

We first review the seismic evidence for attenuation in the various regions of the earth. We then make a parametric investigation of the effects of Q_K and Q_μ (seismic quality factors in compression and in shear) in the mantle and core on the attenuation of normal modes and teleseismic body waves. Next, great circle surface wave and short-period fundamental mode data are combined to obtain global averages for periods of less than 300 s. These data are inverted to obtain Q for the upper mantle. A smooth variation of Q with depth in the lower mantle is adopted based on the near constancy of t^* at teleseismic distances. Finally, we present a family of models and compare their properties with the body wave and normal mode data. The models can be used to normalize body wave, surface wave, and free oscillation data to a common base in order to determine a self-consistent earth model [*Jeffreys*, 1965; *Davies*, 1967; *Akopyan et al.*, 1975; *Liu et al.*, 1976; *Anderson et al.*, 1976; *Hart et al.*, 1976, 1977] and to help in the identification of normal mode spectral peaks [*Gilbert and Dziewonski*, 1975]. The models can also be used to correct seismic data in order to obtain improved estimates of seismic moments.

SURFACE WAVE AND NORMAL MODE DATA

Fundamental mode surface wave and normal mode observations are summarized in Tables 1–8. The general increase in Q with period led *Anderson and Archambeau* [1964] to conclude that Q increases with depth and that this increase should be fairly rapid at some depth greater than 400 km. Unfortunately, the scatter of the data for periods between about 400 and 100 s makes it difficult now, as then, to determine the nature and depth of the transition between the low-Q upper mantle and the high-Q lower mantle.

The overtone data are also difficult to utilize. The observations [*Dratler et al.*, 1971; *Smith*, 1972; *Nowroozi*, 1968, 1974; *Sailor and Dziewonski*, 1975, 1978; *Jobert and Roult*, 1976; *Roult*, 1975; *Deschamps*, 1977; *Buland and Gilbert*, 1978] ex-

Paper number 8B0973.
0148-0227/78/128B-0973$01.00

TABLE 1. Low-Order Fundamental Q Values

Mode	Period,* s	Data †			SL2	SL3	SL7	SL8
		1	2	3				
${}_0S_2$‡	3231.72	589	500	370–589	607	486	600	540
${}_0S_3$‡	2134.00	460	450	450–520	489	400	477	435
${}_0S_4$‡	1545.60	411	400	330–411	462	353	431	398
${}_0S_5$‡	1190.18	352	300	300–400	470	333	418	391
${}_0S_6$	963.54	343	270	273–399	483	320	416	391
${}_0S_7$	812.19	373	460	373–460	487	309	411	392
${}_0S_8$	707.82	357	230	295–457	474	296	403	388
${}_0S_9$	633.95	326	366	284–775	448	282	390	380
${}_0S_{10}$	579.55	329	320	233–329	417	270	375	368
${}_0S_{11}$	537.26	···	254	240–254	389	261	361	355
${}_0S_{12}$	502.72	335	280	200–335	365	254	347	341
${}_0S_{13}$	473.55	305	310	260–310	345	248	333	326
${}_0S_{14}$	448.39	298	403	252–403	328	244	320	313
${}_0T_2$	2630.81	···	250	250–400	309	220	284	272
${}_0T_3$‡	1702.54	···	370	370–400	289	210	266	257
${}_0T_4$‡	1303.72	138	290	118–290	267	200	246	241
${}_0T_5$	1075.55	185	280	161–300	247	190	227	224
${}_0T_6$	925.53	357	280	266–448	229	183	211	209
${}_0T_7$	818.04	125	···	109–141	214	176	197	195
${}_0T_8$	736.41	200	170	170–250	201	171	186	184
${}_0T_9$	671.81	···	180	157–180	191	166	176	175
${}_0T_{10}$	619.11	188	200	173–250	183	162	168	167

*Model 1066A [*Gilbert and Dziewonski*, 1975].

†Sources are 1, *Sailor and Dziewonski* [1978] (spheroidal) or *Bolt and Brillinger* [1975]; and 2, *Smith* [1972] or *Nowroozi* [1974]; column 3 is range of observations given in columns 1 and 2.

‡*Stein and Geller* [1978] have recently determined the following values: ${}_0S_2$, 425–550; ${}_0S_3$, 325–450; ${}_0S_4$, 275–400; ${}_0S_5$, 300–325; ${}_0T_3$, 325; ${}_0T_4$, 425. *Buland and Gilbert* [1978] determined 775–815 for ${}_0S_2$.

hibit considerable scatter and internal inconsistencies. Possible mode misidentifications further complicate the interpretation of these data.

The observed Q for the radial modes (Table 4) are extremely high, suggesting that losses in compression are low. The radial mode Q constitute important data in determining the dissipation in the outer and inner cores.

MM8 is an adequate fit to the Love wave and toroidal mode data and to the Rayleigh wave data, but is not a good fit to the spheroidal or radial mode data [*Anderson and Hart*, 1978]. There are several possible ways to improve the fit: (1) decrease the Q in the lower mantle, (2) include a zone of relatively high dissipation near the core-mantle boundary, (3) introduce a region of bulk dissipation somewhere in the earth, and (4) include the effects of dissipation in the core. There is body wave evidence in support of each of these options. In particular, the effect of the inner core has been neglected in most previous studies.

BODY WAVE DATA

The intrinsic attenuation of seismic waves is difficult to measure because of the other factors which affect amplitudes, such as scattering, geometric spreading, multipathing, source radiation, instrumental uncertainties, radial and lateral inhomogeneities, rotational and ellipticity effects, and mode interference and coupling. These uncertainties, plus the unknown effect of frequency, make the measurement and interpretation of Q difficult. Suitably designed experiments can remove some of these problems, and body wave data are a valuable, and in this study an indispensable, complement to the normal mode data.

The observed decay of near-vertical multiple *ScS* phases provides a simple measure of the average shear wave attenuation in the mantle that is relatively uncontaminated by source, instrument, path, spreading, and local effects. The average mantle Q_β obtained by these observations is appropriate for the period range of about 10–50 s. These data, reviewed by *Anderson and Hart* [1978], provide an integral constraint on Q_β models of the mantle. With somewhat less certainty we can obtain average Q_β values above and below the source [*Anderson and Kovach*, 1964; *Kovach and Anderson*, 1964]. Other techniques [*Kanamori*, 1967*a*, *b*, *c*; *Mikumo and Kurita*, 1968; *Berzon et al.*, 1974] provide constraints for Q_α for certain regions of the mantle.

Published whole mantle values for Q_β range from 156 to 700, with most (66%) of the observations lying between 230 and 380. There are some indications of regional, frequency, and distance effects.

A constraint can be placed on the Q_β of the upper mantle from studies of *sScS* [*Otsuka*, 1962; *Anderson and Kovach*, 1964; *Kovach and Anderson*, 1964; *Steinhart et al.*, 1964; *Yoshida and Tsujiura*, 1975]. These measurements indicate that the mean Q above 600 km is about 168 ± 37, although most of the data refer to the upper mantle beneath South America and Japan and therefore have a strong regional bias. Other integral body wave constraints on mantle Q have been obtained from observations of *PcP* and spectral studies on direct *P* and *S* arrivals. These are summarized by *Anderson and Hart* [1978].

The ratio of body wave travel time T to average Q along the ray for both direct *P* and *S* wave (T/Q_α and T/Q_β) also serves as an important constraint on possible Q models. This is the parameter t_β^* or t_α^* [*Kovach and Anderson*, 1964]. *Carpenter and Flinn* [1965] suggested that for short-period *P* waves the ratio of travel time to the path average of Q is almost constant, about 1 s at teleseismic distances. For frequencies of about 1 Hz, most observed values of t_α^* fall in the range of 0.4–1.3 s [*Carpenter*, 1966; *Mikumo and Kurita*, 1968; *Frazier and Filson*, 1972; *Helmberger*, 1973] with some higher-frequency observations as low as 0.2 [e.g., *Douglas et al.*, 1974]. This latter result plus interpretations of *ScS* spectra by *Yoshida and Tsujiura*

TABLE 2. Fundamental Spheroidal Mode Q

Mode	Period,* s	Data†					SL2	SL3	SL7	SL8
		1	2	3	4	5				
${}_0S_{15}$	426.40	288				227	313	239	306	299
${}_0S_{16}$	406.98	224	278‡			300	300	235	293	286
${}_0S_{17}$	389.69	215				316	288	231	280	273
${}_0S_{18}$	374.19	219				173	278	227	268	262
${}_0S_{19}$	360.20	167				251	268	224	256	251
${}_0S_{20}$	347.50	185		146		250	259	220	245	241
${}_0S_{21}$	355.90	188				222	251	216	234	231
${}_0S_{22}$	325.24	207		167		200	244	213	225	222
${}_0S_{23}$	315.40	200				210	237	210	216	215
${}_0S_{24}$	306.26	201				210	231	206	209	207
${}_0S_{25}$	297.75	185	213	178	198	200	225	203	201	201
${}_0S_{29}$	268.54	175	203	182		164	206	192	178	180
${}_0S_{40}$	212.48	149	155	172	177	149	173	169	146	149
${}_0S_{50}$	178.29	137	155			113	157	155	133	136
${}_0S_{51}$	175.44	135	152	137			156	154	132	135
${}_0S_{57}$	159.99	132	140	123			149	149	129	131
${}_0S_{60}$	153.18	122				110	147	146	127	129
${}_0S_{65}$	142.98	116				137	143	143	125	127
${}_0S_{70}$	133.99	122					140	140	124	125
${}_0S_{76}$	124.52	127					137	137	122	124

*Model 1066A [*Gilbert and Dziewonski*, 1975].

†Sources are 1, *Deschamps* [1977], *Roult* [1975], or *Nowroozi* [1968, 1974]; 2, *Wu* [1972] (average of 16 paths); 3, *Kanamori* [1970] (average of 13 paths); 4, *Ben-Menahem* [1965] (average of 12 paths); and 5, *Sailor and Dziewonski* [1977] or *Smith* [1972].

‡*Buland and Gilbert* [1978].

[1975] indicate that Q may increase with frequency for the shorter-period body waves. Also t_α* decreases with focal depth and may decrease with distance out to 80° [*Mikumo and Kurita*, 1968]. Observed values of t_β* generally range from about 3.5 to 4.5 for the frequency range 0.1–0.05 Hz [*Carpenter and Flinn*, 1965; *Helmberger and Engen*, 1974]. The values appear to be independent of epicentral distance for $20° < \Delta < 80°$ [e.g., *Hart and Butler*, 1977], but they do depend on source depth. *Burdick* [1977] determined t_β* to be 5.2 ± 0.7 s from the shallow Borrego Mountain (California) earthquake and 3.0 ± 0.5 s for deep focus events (537–598 km). This is an indication that Q of the lower mantle is higher than that of the upper mantle, which supports the conclusions drawn from *ScS* and surface wave studies.

Because of the large regional variations in Q for surface waves and the lack of precise and consistent data in the period range between 300 and 600 s, it is difficult to determine the gradient of Q in the lower mantle. A constant t* at teleseismic distances implies a smoothly increasing Q with depth. This is a constraint we adopt later and test against the mode data.

The Lowermost Mantle and Core

Body wave data serve as particularly important constraints on the lowermost mantle and the core. The normal mode data alone are far too ambiguous to resolve some important features of these regions.

A large number of body wave observations are consistent with a low-Q zone at the base of the mantle. *Mikumo and Kurita* [1968] observed an increase in T/Q_α at distances beyond 85°. Such an increase implies a decrease of Q_α in the lowermost mantle. Their model has a 300-km-thick layer at the base of the mantle with $Q_\alpha \sim 100$. *Teng* [1968] determined the variation of Q_α with depth from the spectra of P phases from deep earthquakes. His data indicate the presence of a 200-km-thick zone with $Q_\alpha \sim 200$. The observed amplitude ratios of *ScS/S* of Mitchell and Helmberger [1973] can be interpreted in terms of a thin low-Q zone (approximately 150 km thick with Q_β of about 100). The amplitudes of grazing *PKP* phases [*Sacks and Snoke*, 1976] also indicate a low-Q zone at the base of the mantle. *Kuster* [1972] proposed a low-Q zone ($Q_\alpha = 300$, thickness equals 150 km) on the basis of *PKP* and *PKKP* spectral amplitude ratios. These studies involve a wide range of wave types, periods, and angles of incidence through the mantle, and in some cases the effect of diffraction is small or explicitly allowed for. In our parametric investigations we will therefore explore the effects of a lowermost mantle low-Q zone, and in our inversions we will allow such models. It should be kept in mind that the lowermost mantle is a strong scatterer, at least for short-period P waves, and the body wave results may reflect this as well as diffraction effects due to the proximity to the core.

The Q of the outer core is apparently extremely high. High-frequency *PmKP* phases (*PKP*, *PKKP*, *PKKKP*, etc.) travel with little change in shape of amplitude for long distances. *Cormier and Richards* [1976] conclude that Q_α in the outer core is at least 10^4 and probably much higher. A high Q for the outer core is supported by studies by *Buchbinder* (1971), *Sacks* [1971*a*, 1972], *Adams* [1972], *Muller* [1973] and *Qamar and Eisenberg* [1974]. Most of these studies infer a Q of greater than 4000.

We are aware of five body wave measurements of the dissipation in the inner core. *Buchbinder* [1971], using *PKP* amplitude ratios, found an average inner core Q of about 400. Spectral ratios of inner core and outer core phases [*Sacks*, 1971*b*] indicate an average inner core Q_α of 600. Sacks' data suggest that Q_α is not constant through the inner core but ranges from 100 to 200 in the outer 300 km to 1000 at greater depths. *Qamar and Eisenberg* [1974] determined a value between 120 and 400 for Q_α in the outer 450 km of the inner core. *Doornbos* [1974] found that Q rises from a value of about 200 near the inner core–outer core boundary to about 600 at a depth of 400 km inside the inner core. *Kuster* [1972] found a

TABLE 3. Fundamental Toroidal Mode Q

Mode	Period,* s	Data†				SL2	SL3	SL7	SL8
		1	2	3	4				
${}_0T_{11}$	575.08	258	270	260		176	158	161	160
${}_0T_{12}$	537.63		189	150–220		171	155	155	155
${}_0T_{13}$	505.28		204	190–260	118–258	166	153	150	150
${}_0T_{14}$	476.99	220	200	135–200		161	150	145	145
${}_0T_{15}$	451.98	240	157	172	158–186	158	148	141	142
${}_0T_{16}$	429.67	174	149	215	185–245	155	146	138	139
${}_0T_{17}$	409.63	163	127	126		152	144	135	136
${}_0T_{18}$	391.49	116	111	188–270	172–204	150	143	133	134
${}_0T_{19}$	374.98	81–94	105	281		147	142	131	131
${}_0T_{20}$	359.88	81		249	97	145	140	129	129
${}_0T_{21}$	346.00	86–111	105	170		144	139	127	128
${}_0T_{22}$	333.18	95–207	108		114	142	138	125	126
${}_0T_{23}$	321.32	91–111	115		123–160	141	137	124	125
${}_0T_{24}$	310.29	123–153	116			139	136	123	124
${}_0T_{25}$	300.01	123	116		104–149	138	135	122	123
${}_0T_{26}$	290.41	97–209				137	134	121	122
${}_0T_{27}$	281.41	93–146	115			136	134	120	121
${}_0T_{28}$	272.96	92–221	116		110	135	133	119	120
${}_0T_{29}$	265.00	95–147	114			135	132	118	119
${}_0T_{30}$	257.50	120–184	115		111–142	134	132	117	119
${}_0T_{31}$	250.42	96–104	110		105	133	131	117	118
${}_0T_{32}$	243.72	106–176	114		133	133	131	116	117
${}_0T_{33}$	237.37	94	108			132	130	116	117
${}_0T_{34}$	231.34	101–167	114			131	130	115	116
${}_0T_{35}$	225.61	105	108		102	131	130	115	116
${}_0T_{36}$	220.16	139–162	115		131	130	129	114	116
${}_0T_{37}$	214.96	93–142				130	129	114	115
${}_0T_{38}$	210.00	111–169				129	128	114	115
${}_0T_{39}$	205.27	95–137				129	128	113	115
${}_0T_{40}$	200.75		118		102–133	129	128	113	114
${}_0T_{45}$	180.81	104–123	115		117	127	127	112	113
${}_0T_{50}$	164.47	93–130	108			126	126	111	112
${}_0T_{55}$	150.82	114–122	108		114–118	125	125	111	112
${}_0T_{60}$	139.26	103–112	104			125	124	110	111
${}_0T_{65}$	129.33		108			124	124	110	111
${}_0T_{70}$	120.73	100	99		116	124	124	110	111
${}_0T_{75}$	113.91	95–140	113			124	123	110	111
${}_0T_{80}$	106.53	86–121	109			123	123	110	111
${}_0T_{85}$	100.62				108	123	123	110	111
${}_0T_{110}$	78.73				109	124	124	111	111

*Model 1066A [*Gilbert and Dziewonski*, 1975].

†Sources are 1, *Roult* [1975]; 2, *Deschamps* [1977]; 3, *Smith* [1961, 1972], *Bolt and Brillinger* [1975], *Nowroozi* [1968], and *Jobert and Roult* [1976]; and 4, *Ben-Menahem* [1965], *Kanamori* [1970], and *Sailor and Dziewonski* [1977].

value of 300 for Q_α from spectral ratios of core phases. In the following we test models in which dissipation is negligible in both the outer and the inner core and models supported by the above studies in which the inner core contributes significant attenuation.

Julian et al. [1972] estimate that Q_μ in the inner core is between 500 and 1000. A high value for Q_μ in this region is also implied by the fact that inner core shear modes (e.g., ${}_2S_2$) are observed [*Buland and Gilbert*, 1978]. The Q of ${}_2S_2$ implies a Q_μ for the inner core of about 550.

Forward Calculations

A variety of simple models and variants of model MM8 were constructed to give the reader a feel for the effects of various parameters. To a first approximation, the Q structure of the earth can be represented by a high-Q lithosphere, a low-Q upper mantle, a higher-Q lower mantle, a nonabsorbing outer core, and an attenuating inner core. There may be a very low Q channel in the uppermost mantle and a low-Q transition region at the base of the mantle. These are characteristics of the earth determined from body wave studies. One object of the present study is to see if they are compatible with the longer-period global data represented by the normal mode data set.

The models consist of an arbitrary number of homogeneous spherical shells. Within each shell we specify either Q_α and Q_β or Q_K and Q_μ. These quality factors are related by the following equations:

$$Q_\beta = Q_\mu \tag{1}$$

$$Q_\alpha^{-1} = LQ_\mu^{-1} + (1 - L)Q_K^{-1} \tag{2}$$

$$Q_K = \frac{(1 - L)Q_\alpha Q_\beta}{Q_\beta - LQ_\alpha} \tag{3}$$

where $L = (4/3)(\beta/\alpha)^2$ and α and β are the compressional and shear velocities, respectively. Q_μ and Q_K are the quality factors

TABLE 4. Q of Radial Modes

Mode	Period,* s	QBS†	SL2	SL3	SL7	SL8	Data‡
${}_0S_0$	1,230.07	4,271	5,141	4,553	4,508	4,374	12,000
							7,500
							7,470
							4,229
							3,996
							900
${}_1S_0$	613.70	2,078	1,475	1,168	1,294	1,180	5,160
							1,970
${}_2S_0$	398.51	1,364	1,220	893	1,059	1,024	1,170
							1,059
							870
							704
							672
${}_3S_0$	305.74	1,100	947	875	912	851	992
							874
${}_4S_0$	243.71	918	1,171	898	978	945	1,264
							1,173
							1,156
							989
							790
							750
${}_5S_0$	204.85	896	1,044	935	970	947	1,570
							942
							938
							927
							824
${}_6S_0$	174.25	1,058	1,173	950	1,093	1,057	933

*Model 1066A [*Gilbert and Dziewonski*, 1975].
†*Sailor and Dziewonski* [1978].
‡*Ness et al.* [1961], *Smith* [1961, 1972], *Slichter* [1967], *Dratler et al.* [1971], *Buland and Gilbert* [1978], and *Sailor and Dziewonski* [1978].

TABLE 5. First Toroidal Overtone Q

						Data†	
Mode	Period,* s	SL2	SL3	SL7	SL8	1	2
${}_1T_7$	474.70	306	220	272	262	238	
${}_1T_9$	407.23	291	208	254	250	178	
${}_1T_{11}$	358.92	271	198	239	238	176	176–249
${}_1T_{12}$	339.49	262	194	233	232	195	
${}_1T_{19}$	249.62	217	177	206	204	141	151–208
${}_1T_{22}$	225.32	206	173	196	194	133	133–172
${}_1T_{23}$	218.38	202	171	193	190	149	139–182
${}_1T_{24}$	211.92	199	170	190	187	164	124–164
${}_1T_{25}$	205.89	196	169	187	184	192	192–286
${}_1T_{26}$	200.26	194	167	183	181	227	202–227
${}_1T_{27}$	194.98	190	166	180	178	222	222–300
${}_1T_{28}$	190.02	188	165	178	175	208	155–284
${}_1T_{29}$	185.36	185	164	178	173	208	172–208
${}_1T_{30}$	180.97	183	163	172	170	189	165–207
${}_1T_{31}$	176.82	181	162	170	168	179	
${}_1T_{32}$	172.89	179	161	167	166	182	173–191
${}_1T_{33}$	169.17	177	160	165	163	192	
${}_1T_{34}$	165.63	176	159	162	161	192	155–192
${}_1T_{35}$	162.27	174	158	161	159	192	172–255
${}_1T_{36}$	159.07	172	158	159	158	200	145–249
${}_1T_{37}$	156.01	171	157	157	156	196	147–239
${}_1T_{38}$	153.10	169	156	155	154	185	169–310
${}_1T_{39}$	150.30	168	156	153	153	179	134–245
${}_1T_{40}$	147.63	167	155	152	151	175	163–180
${}_1T_{41}$	145.06	166	154	150	150	161	145–179
${}_1T_{42}$	142.59	165	154	148	148	159	152–209
${}_1T_{43}$	140.22	164	153	147	147	161	122–193
${}_1T_{44}$	137.93	163	153	146	146	161	145–173
${}_1T_{45}$	135.73	162	152	145	145	167	151–202
${}_1T_{50}$	125.80	158	150	140	140	152	122–193
${}_1T_{55}$	117.33	155	149	135	136	135	
${}_1T_{59}$	111.38	153	147	132	134	134	
${}_1T_{61}$	108.64	152	147	131	132	138	

*Model 1066A [*Gilbert and Dziewonski*, 1975].
†Column 1 data are from *Deschamps* [1977] and *Jobert and Roult* [1976]. Range of data (from column 1 and sources given in the text).

TABLE 6. Toroidal Overtone Q

Mode	Period,* s	SL2	SL3	SL7	SL8	Data†
${}_2T_2$	447.57	288	205	232	197	320
${}_2T_{36}$	133.12	219	176	217	214	183
${}_2T_{37}$	130.58	216	176	214	212	172
${}_2T_{46}$	111.88	197	168	192	190	189
${}_2T_{47}$	110.19	195	168	190	187	182
${}_2T_{49}$	106.99	191	166	185	181	207
${}_2T_{51}$	104.01	188	165	180	175	178
${}_2T_{52}$	102.60	186	164	178	172	162
${}_2T_{54}$	99.92	183	162	173	172	144
${}_2T_{62}$	90.79	172	157	160	159	143
${}_3T_{26}$	147.11	309	203	260	241	264
${}_3T_{27}$	143.66	304	202	258	240	296
${}_3T_{30}$	134.27	290	198	252	239	215
${}_3T_{53}$	91.02	219	176	217	214	236
${}_4T_{11}$	200.02	261	210	245	247	208
${}_4T_{17}$	170.29	257	226	259	254	204
${}_5T_9$	174.62	260	201	240	219	243

*Model 1066A [*Gilbert and Dziewonski*, 1975].
†*Roult* [1975], *Smith* [1972], and *Sailor and Dziewonski* [1978].

in pure shear and pure compression. Since Q_μ and Q_K must be positive, Q_α and Q_β must satisfy

$$Q_\beta/Q_\alpha \geq L \tag{4}$$

When Q_K^{-1} is identically zero, i.e., all losses occur in shear, the ratio of Q_β to Q_α is equal to L. Larger ratios occur when finite dissipation occurs due to bulk modulus relaxation. Such losses occur, for example, if phase changes or intergranular thermoelastic effects contribute significantly to the attenuation. We have examined and discuss below the consequences of assuming finite Q_K^{-1} values in the earth.

For a given distribution of Q versus depth the mode Q is [*Anderson et al.*, 1965]

Toroidal

$$Q_T^{-1} = \sum_{l=1}^{N} \frac{\beta_l}{C_T}\left(\frac{\partial C_T}{\partial \beta_l}\right)_{K,\rho,\beta} Q_{\beta_l}^{-1} \tag{5}$$

Spheroidal

$$Q_S^{-1} = \sum_{l=1}^{N} \left[\frac{\alpha_l}{C_S}\left(\frac{\partial C_S}{\partial \alpha_l}\right)_{K,\rho,\beta} Q_{\alpha_l}^{-1} + \frac{\beta_l}{C_S}\left(\frac{\partial C_S}{\partial \beta_l}\right)_{K,\rho,\alpha} Q_{\beta_l}^{-1}\right] \tag{6}$$

In (5) and (6), ρ is the density, C is the phase velocity or frequency, subscript l is the layer or shell index, and subscripts S, T, α, and β associated with Q refer to the modes or wave type. Other subscripts refer to the quantities being held constant. The density ρ is real, while α and β are complex. The equations can be used to relate modal and layer Q in both the forward and inverse problems.

The parameters of interest in the simple earth models are Q_μ and Q_K in each shell and the location of the boundaries. We are particularly interested in the thickness of the upper mantle low-Q region, the effects of a low-Q transition zone at the base of the mantle, a low-Q inner core, and finite Q_K^{-1}. We therefore do a series of parametric calculations. The results are summarized in a series of figures for the toroidal, spheroidal, and radial modes.

PARAMETRIC Q MODELS

The main defect of model MM8 is the predicted high Q relative to published observations for the low-order spheroidal modes and the radial modes [*Anderson and Hart*, 1978]. One way to decrease these values is by decreasing the average Q_β of the mantle. We take several simple starting models which have low-Q upper mantles and high-Q lower mantles and decrease the average mantle Q by increasing the depth to the transition and by decreasing the Q of the lower mantle. The basic models are given in Tables 9 and 10. The models have a high-Q lithosphere, a low-Q upper mantle, and a high-Q lower mantle. In these models there is no dissipation in the core, and all dissipation occurs in shear, i.e., $Q_K = \infty$. Figure 1 shows the Q of the three mode types as a function of depth to the transition and the average mantle Q_β. The low-order spheroidal modes are brought into an acceptable range for a thick (>1000 km) low-Q upper mantle, but the radial mode Q are too high (cf. Table 4). Also t_α^* and t_β^* are greater than 1.4 and 6.4 s, respectively, at 40°.

One way to bring the radial modes Q down is to introduce bulk dissipation. Numerical experiments show that even a small K^*/μ^* throughout the mantle is unacceptable. However, a finite K^*/μ^* ratio in the upper mantle has a large effect on the radial modes and only a small effect on the spheroidal modes. Figure 2 shows the effect of finite K^*/μ^* in the upper

TABLE 7. Q of Spheroidal Overtones

Mode	Period,* s	SL2	SL3	SL7	SL8	Data†
${}_2S_{15}$	308.92	297	258	266	252	244
${}_2S_{23}$	202.08	387	474	571	407	514
${}_2S_{26}$	179.21	216	193	206	202	158–275
${}_2S_{30}$	160.62	193	171	180	179	150–207
${}_2S_{31}$	156.61	191	179	179	178	143
${}_2S_{39}$	131.05	179	161	172	169	179
${}_2S_{57}$	97.60	170	155	163	160	174
${}_2S_{60}$	93.83	168	154	159	158	151
${}_3S_{12}$	297.35	307	227	270	261	179–239
${}_3S_{13}$	285.05	300	222	262	255	227–271
${}_3S_{14}$	273.43	290	218	254	249	274
${}_3S_{15}$	262.43	281	213	245	242	163–394
${}_3S_{16}$	252.11	271	209	237	236	259–285
${}_3S_{18}$	233.38	253	201	224	223	157–232
${}_3S_{20}$	217.00	237	194	212	212	229
${}_3S_{42}$	111.43	225	187	211	211	180
${}_4S_3$	488.38	590	434	557	534	560
${}_4S_{14}$	225.24	332	240	304	296	288
${}_4S_{19}$	192.06	344	226	301	294	291
${}_4S_{21}$	180.71	343	221	298	291	275
${}_4S_{23}$	170.45	336	219	293	287	312
${}_4S_{25}$	161.21	324	216	286	281	260
${}_4S_{26}$	156.95	319	214	282	278	306
${}_4S_{31}$	138.75	284	205	259	258	264
${}_4S_{32}$	135.65	278	204	254	254	299
${}_4S_{34}$	129.88	265	200	245	245	219–234
${}_4S_{35}$	127.19	259	199	240	240	246
${}_4S_{39}$	117.61	238	192	222	223	193
${}_5S_{22}$	154.37	358	236	310	303	306–346
${}_5S_{24}$	146.94	355	231	302	298	308–339
${}_5S_{25}$	143.48	351	229	298	294	231–433
${}_5S_{26}$	140.18	347	226	293	291	236–299
${}_5S_{30}$	128.51	324	219	277	276	248
${}_5S_{38}$	110.61	293	210	265	263	223
${}_6S_1$	505.47	1002	649	893	873	613–700
${}_6S_8$	267.93	281	283	275	263	286
${}_6S_9$	252.47	341	327	325	314	292
${}_6S_{13}$	191.19	304	249	273	264	291
${}_6S_{23}$	138.16	375	283	332	325	186–299
${}_6S_{26}$	128.86	371	259	320	249	368
${}_6S_{31}$	116.33	375	242	314	244	391
${}_6S_{36}$	105.95	368	236	308	247	342
${}_6S_{47}$	88.87	308	221	264	237	276

*Model 1066A [*Gilbert and Dziewonski*, 1975].
†Range of data (see text for data sources).

TABLE 8. High-Q Modes

Mode	Period,* s	Data†	SL2	SL3	SL7	SL8
${}_1S_7$	604.18	484	599	315	498	473
${}_2S_2$	1049.00	546	299	298	577	544
${}_2S_{23}$	202.08	.514	387	474	571	407
${}_3S_1$	1060.82	1020	1001	774	964	902
${}_4S_3$	488.38	560	590	434	557	534
${}_4S_{23}$	170.45	312	336	219	293	287
${}_4S_{26}$	156.95	306	319	214	282	278
${}_5S_7$	303.76	496	717	442	592	589
${}_6S_1$	505.47	613–700	1051	649	893	873
${}_8S_1$	348.31	704	1108	861	1023	1004
${}_8S_9$	192.02	483	485	466	516	477
${}_{10}S_2$	247.85	870	860	699	887	853
${}_{10}S_{28}$	95.61	399	361	292	348	332
${}_{11}S_3$	224.05	368–696	631	442	546	533
${}_{11}S_4$	209.62	652	1095	720	920	904
${}_{13}S_1$	228.48	574–1573	968	767	841	824
${}_{13}S_2$	206.50	1125	1090	891	960	941
${}_{16}S_{20}$	88.77	463	737	503	619	604
${}_{17}S_{24}$	79.82	435	583	450	521	515
${}_{19}S_{13}$	95.89	496	633	536	597	581
${}_{20}S_{18}$	83.19	630	840	596	723	712

*Model 1066A [*Gilbert and Dziewonski*, 1975].
†*Sailor and Dziewonski* [1978], *Buland and Gilbert* [1978], *Nowroozi* [1974], and *Dratler et al.* [1971].

mantle on the radial and spheroidal modes with and without inner core dissipation. The basic model is given in Table 10. A relatively large K^*/μ^* ($\sim\frac{1}{2}$) brings ${}_0S_0$ into agreement with the data, but the radial overtones are still too high. With inner core dissipation in shear the radial modes are in better agreement with the data for relatively small bulk dissipation in the upper mantle.

In these models, dissipation in the inner core is entirely in shear. We will show later that by allowing for bulk losses in the inner core we can satisfy radial mode, core mode, and body wave data with no bulk dissipation in the mantle.

Figure 3 shows the effect on the radial modes of the depth of the transition for a model with inner core dissipation, with and without upper mantle bulk dissipation. Series C has only shear dissipation, and series D has $K^* = \mu^*/8$ in the upper mantle. Also indicated is the average mantle Q. The basic model is again given in Table 10. Both series suggest that the transition from low-Q upper mantle to high-Q lower mantle occurs below some 800 km. However, t_α^* is greater than 1.2 s in the distance range between 30° and 90° for models having this amount of bulk dissipation above 800 km. The models with no bulk dissipation in the upper mantle give t_α^* of about 1.02 s, consistent with the body wave data.

An alternate way to decrease the values of Q of the low-order spheroidal modes is by the introduction of a low-Q zone at the base of the mantle, as suggested by body wave studies. Figure 4 shows the effect of a low-Q (Q_μ = 100) zone at the base of the mantle as a function of its thickness. The model parameters are given in Table 9. Note the dramatic effect of even a relatively thin low-Q zone on the low-order spheroidal modes and the odd-numbered radial overtones. The even-numbered radial modes, the high-order spheroidal modes, and the toroidal modes are not much affected. Note that some other perturbation is still required to the basic model in order to satisfy the radial mode data. It should be pointed out that the Q values for the low-order spheroidal models are still uncertain.

It appears that bulk dissipation somewhere in the earth is required by the radial mode data. We now investigate the effect of finite Q_K in the inner core. We start with a two-layer inner core with Q_α of 400 and 1000, respectively, in the outer and inner half and vary Q_μ and Q_K, maintaining these values of Q_α which are suggested by the *PKIKP* data. Figure 5 shows the radial mode Q as a function of Q_μ and Q_K of the outer half of the inner core. Note that $Q_K \sim Q_\mu$ gives good agreement. If the observed attenuation of *PKIKP* is all in shear, then not only are the radial mode data violated, but an extremely low Q_μ is implied. This would be inconsistent with both the observation of inner core shear modes and the values inferred for inner core Q_μ by *Julian et al.* [1972]. On the basis of this evidence we conclude that the source of the required bulk dissipation probably resides in the inner core.

TABLE 9. Models With Variable Thickness Low-Q Zone at Base of Mantle and Inner Core Dissipation in both Bulk and Shear (Series A and B)

Depth, km	Q_β Series A	Q_β Series B
0–45	1500	1500
45–79	200	200
79–148	85	85
148–353	110–150	110–150
353–1626	200–500	200–500
1626–1800	600–800	500
Lower mantle	2000	500
Low-Q zone	100	100
Outer core	$Q_K = \infty$	
Inner core	Q_μ = 200–600 Q_α = 450–900	

NORMAL MODE Q DATA

A fairly complete summary of published normal mode Q data is given in Tables 1–8. In many cases the mode designations given by the original authors are based on period alone. On the basis of excitation calculations many of the assignments are clearly in error, and we have made some redesignations; see, for example, *Anderson and Hart* [1978]. The tables also give theoretical values for two models, SL2 and SL3, derived by *Anderson and Hart* [1978] and other models to be discussed later.

In model SL2 an attempt was made to satisfy the t^* body wave attenuation data discussed earlier. The constancy of t^* as a function of distance leads to models with Q increasing with depth. SL2 provides a more or less upper bound to the longer-period spheroidal mode data. It has a low-Q zone at the base of the mantle, inserted to decrease the Q of the spheroidal modes at long period. In model SL3 this same purpose was

TABLE 10. Models Showing the Effect of Varying the Thickness of the Low-Q Upper Mantle and Finite Q_K in the Upper Mantle (Series C and D)

Depth, km	Q_β (Series C and D)	Q_K* (Series D)
0–45	1500	∞
45–79	200	1600
79–h	125	1000
Lower mantle	400	∞

*$Q_K = Q_\mu/8$ in upper mantle; core is same as that in series A and B; $Q_K = \infty$ in mantle for series C; h is depth to top of lower mantle.

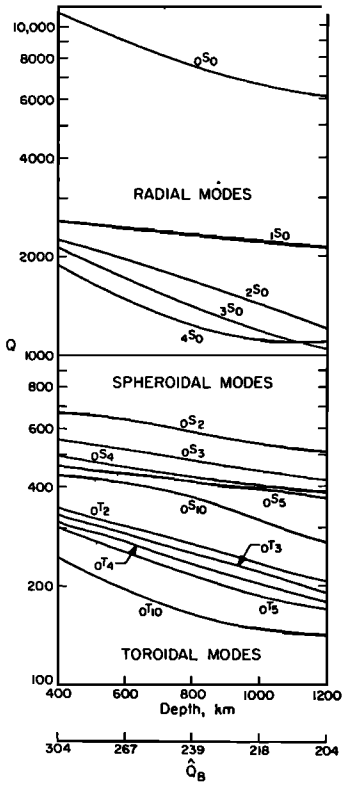

Fig. 1. Relationship between average mantle Q_β and modal Q of radial, spheroidal, and toroidal modes. 'Depth' is the location of the boundary between the low-Q upper mantle and higher-Q (400) lower mantle. All losses are in shear, and there is no dissipation in the core.

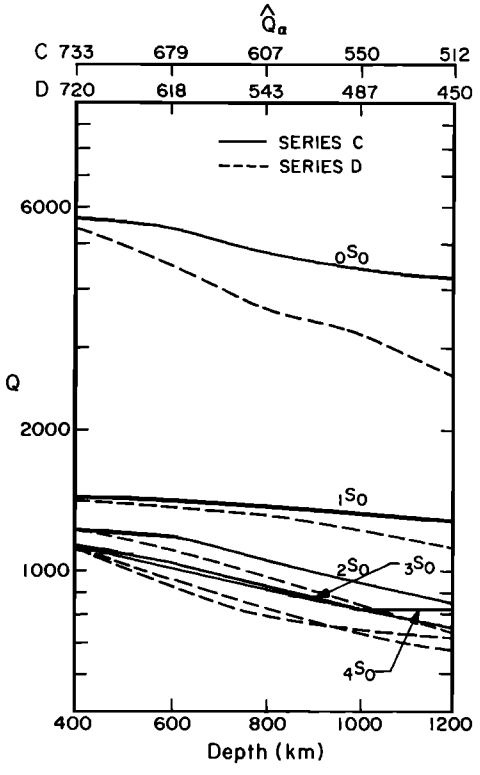

Fig. 3. Effect of depth of low-Q upper mantle layer on radial modes. Series C has only shear dissipation in the mantle; series D has $K^* = \mu^*/8$ in the upper mantle. Inner core has shear dissipation only.

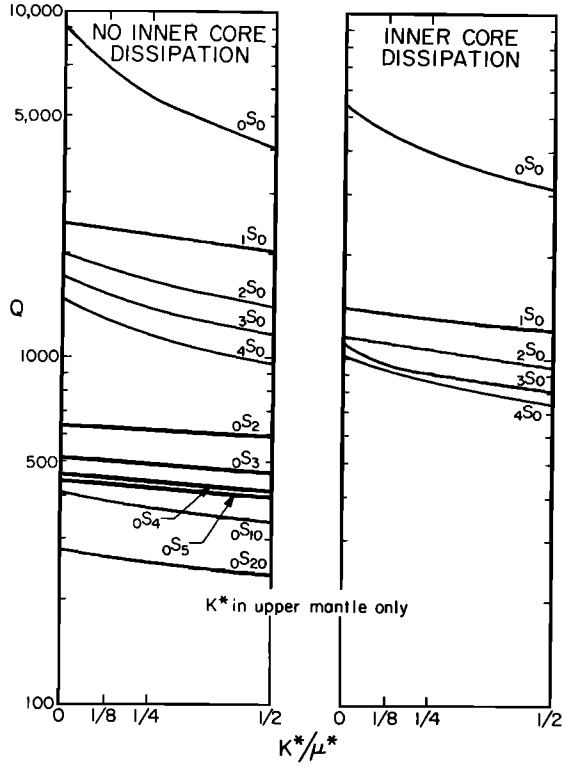

Fig. 2. Effect of finite K^* in the upper mantle on radial and spheroidal modes with and without inner core dissipation. K^* and μ^* are the imaginary parts of the bulk modulus and rigidity. $Q_\alpha = [K + (4/3)\mu]/[K^* + (4/3)\mu^*]$, and $Q_\beta = Q_\mu = \mu/\mu^*$.

accomplished by decreasing the Q of the whole lower mantle. This model provides a rough lower bound allowable by the spheroidal data for periods greater than about 600 s. SL3 has unacceptable t_α^* (Table 13) both in absolute value and in the variation with distance. Both models are too high to satisfy the shorter-period data, indicating a frequency dependence of Q or a more attenuating upper mantle. The latter alternative is tested below. In a later paper we give frequency dependent Q models.

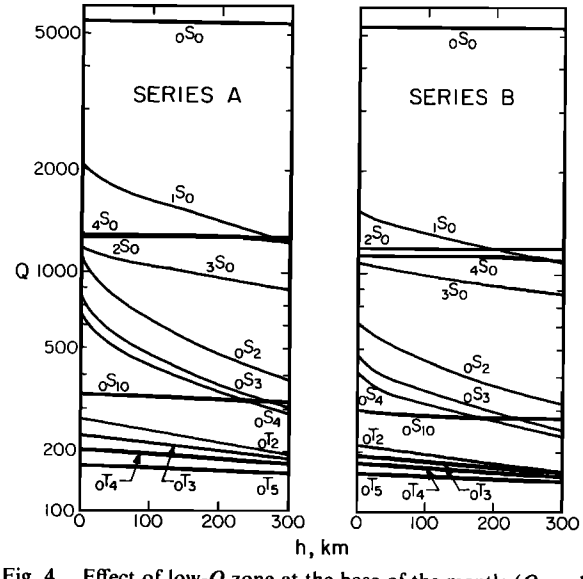

Fig. 4. Effect of low-Q zone at the base of the mantle ($Q_\beta = 100$) on low-order radial, spheroidal, and toroidal modes, as a function of thickness h of low-Q zone.

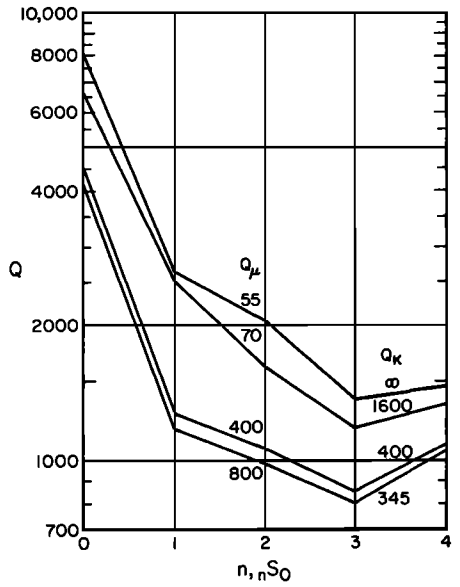

Fig. 5. Effect of Q_μ and Q_K for fixed Q_α of inner core on radial modes.

Q MODELS

As mentioned earlier, there is considerable scatter and ambiguity in the normal mode Q data. Fortunately, there is a considerable amount of short-period Love and Rayleigh wave data, and trends which are hidden by the scatter of individual observations become evident when groups of modes are considered. We are initially interested in the Q structure of the upper mantle. Modes which are sensitive to Q_β of the upper mantle and for which many observations are available are summarized in Table 11. Also given is the depth region to which they are most sensitive. At least 50% of the data have values in the range given. The mode groupings were picked on the basis of available data and have 10% or less variation in theoretical Q over the range of modes considered. Although there is overlap in the observed values between adjacent mode groups, there is a tendency for the observed values to increase with period for a given mode. It is also clear, upon examination of the depth range of sensitivity, that Q_β increases from 420 to 670 km and also from 200 to 670 km. Models having constant Q above 670 km do not satisfy these trends. The near constancy of t^* between 30° and 80° or the small decrease over this range [*Mikumo and Kurita*, 1968] indicates that Q continues to increase below 670 km to some depth above the core-mantle boundary. Therefore a realistic Q model for the earth must involve a general increase of Q with depth below some 200 km.

Rather than attempt to invert the normal mode data directly as an independent data set, we prefer, at this point, to test its consistency with inferences from other sources and to determine what, if any, additional information is available. The final model, found by successive approximations, is compatible with the data, but no claim is made that it is unique.

Our first step was to take the relatively smooth model SL2 from *Anderson and Hart* [1978] and adjust large areas of the mantle in order to match the modal data and retain agreement with body wave data. The result was model SL7. This model was then smoothed and iterated until a satisfactory fit to all data was achieved. This gave model SL8, which is our preferred frequency independent model. Parameters are given in Tables 14 and 15; comparisons with the data, along with models SL2 and SL3, are in Tables 1–13. Model SL8 is shown in Figure 6. Results are given in some cases for the four-layer Q model QBS of *Sailor and Dziewonski* [1978]. Model SL8 is discussed below. The models are given in Tables 14 and 15.

Q_K is infinite in the whole mantle; i.e., all losses are in shear. Q_α decreases slightly in constant Q_β regions of the mantle because of the α/β effect on the relation of the two (equation (2)). These decreases are not significant.

Model SL8 has a 45-km-thick 'lithosphere' with relatively high Q (Q_β = 500, $Q_\alpha \sim$ 1100). A low-Q channel (Q_β = 90) occurs between 79 and 148 km. Q_β remains low (105) down to 353 km. It then increases smoothly to 515 at 2235-km depth, where it levels off and then decreases at the base of the mantle. This trend keeps t_α^* relatively constant from 30° to 80°, at which point it starts to increase rapidly as required by the body wave data.

The high value of Q_β for the lithosphere is supported by the short-period observations of *Tsai and Aki* [1969], *Press* [1964], *Bhattacharya* [1975], and *Mitchell* [1973]. These studies also indicate a smaller Q (~200) in the uppermost lithosphere, an effect beyond the resolution of the data we have used. The high average Q of the lithosphere is a consequence of its low temperatures. The lower Q at its top is presumably due to cracks and volatiles.

We now reconsider the question of bulk dissipation in the mantle. We have already shown that bulk dissipation in the inner core is consistent with the radial mode data. Some high-Q overtones have been observed which have a relatively high sensitivity to compressional losses. These are given in Table 8. Also given are model values. Model SL8, having only shear

TABLE 11. Range of Q for Selected Model Groups

	Number of Observations	Mode Q			
		Data*	QBS†	SL8	Region, km
${}_0T_{18}$–${}_0T_{28}$	22	105–126	122–130	122–134	above 670
${}_0T_{27}$–${}_0T_{110}$	71	102–118	122–127	111–121	above 420
${}_1T_{36}$–${}_1T_{44}$	14	145–161	130–144	146–158	200–670
${}_1T_{45}$–${}_1T_{64}$	14	134–154	119–129	130–145	200–670
${}_0S_{25}$–${}_0S_{28}$	21	175–200	153–165	184–201	above 670
${}_0S_{29}$–${}_0S_{35}$	20	164–203	138–150	160–180	above 670
${}_0S_{37}$–${}_0S_{45}$	19	139–151	130–135	141–155	above 420
${}_0S_{50}$–${}_0S_{57}$	17	132–152	128–129	131–136	above 420

* 50% of data included in this range.
†*Sailor and Dziewonski* [1978].

TABLE 12. Average Mantle Q

Depth, km	SL2		SL3		SL7		SL8	
	$\bar{Q}_\beta$	$\bar{Q}_\alpha$	$\bar{Q}_\beta$	$\bar{Q}_\alpha$	$\bar{Q}_\beta$	$\bar{Q}_\alpha$	$\bar{Q}_\beta$	$\bar{Q}_\alpha$
0–671	147	374	144	365	128	325	130	328
671–2886	415	1047	258	645	396	998	360	912
0–2886	268	678	208	524	243	615	235	593

dissipation in the mantle, is not consistently higher than the observations, as one would expect if there were bulk dissipation processes in the mantle. In fact, it is lower than the observations in half the cases. Most of the data (57%) is satisfied to within ±15%, an estimate of the data uncertainty if the modes have been correctly identified, by model SL8. We conclude that there is no evidence for bulk dissipation in the mantle and that the bulk dissipation required by the radial modes is probably in the inner core, substantiating conclusions reached earlier on different grounds.

The average Q_β of the mantle for model SL8 is 235. This is within the range of the published *ScS* Q data discussed earlier and is near the bottom of the range which encompasses 66% of the data. It is much lower than the majority of data from continents but is close to the values measured in some oceanic and tectonic regions (see summary by *Anderson and Hart* [1978]). It is close to values measured for the southwestern United States (230), Hawaii (230), the Solomon Islands (230), and some values measured for Japan (260). Since the data used in the present paper represent global means, the implication is that the mantle under oceans is more attenuating than it is under continents.

TABLE 13. Parameters t_α^* and t_β^*

Δ, deg	Surface Focus (0 km)		Intermediate Focus (110 km)		Deep Focus (600 km)	
	t_α^*	t_β^*	t_α^*	t_β^*	t_α^*	t_β^*
			Model SL2			
30	0.83	3.79	0.79	3.65	0.64	2.82
40	0.95	4.28	0.91	4.14	0.76	3.35
50	0.99	4.57	0.95	4.32	0.75	3.49
60	0.97	4.58	0.93	4.42	0.74	3.52
70	0.90	4.42	0.86	4.27	0.67	3.20
80	0.83	3.97	0.79	3.75	0.60	2.93
90	0.92	3.82	0.88	3.63	0.97	2.79
			Model SL3			
30	0.91	4.13	0.87	4.01	0.73	3.31
40	1.08	4.88	1.05	4.76	0.91	4.05
50	1.21	5.57	1.18	5.32	1.01	4.56
60	1.28	5.95	1.25	5.82	1.08	4.98
70	1.33	6.27	1.29	6.13	1.12	5.22
80	1.35	6.33	1.32	6.15	1.13	5.39
90	1.33	6.45	1.29	6.25	1.12	5.44
			Model SL7			
30	0.90	4.12	0.86	3.94	0.67	2.89
40	1.00	4.51	0.95	4.33	0.75	3.26
50	1.01	4.63	0.96	4.39	0.75	3.41
60	1.04	4.82	1.00	4.63	0.80	3.69
70	1.06	5.07	1.02	4.88	0.81	3.81
80	1.05	4.94	1.00	4.71	0.79	3.79
90	1.03	4.96	0.99	4.74	0.83	3.81
			Model SL8			
30	0.91	4.15	0.86	3.97	0.68	2.98
40	1.02	4.61	0.97	4.43	0.79	3.42
50	1.04	4.77	0.99	4.50	0.76	3.50
60	1.04	4.82	0.99	4.63	0.79	3.65
70	1.06	4.93	1.01	4.75	0.81	3.78
80	1.06	4.99	1.01	4.77	0.82	3.87
90	1.12	5.07	1.07	4.87	0.96	3.97

The upper mantle Q_β for model SL8 is 130. This again is in the range of published observations and again is at the lower end of the majority of the data. This reinforces the conclusion just drawn. Average values of Q and t^* results are given in Tables 12 and 13 for the models discussed in this paper.

Sailor and Dziewonski [1978] used 38 modes to determine a relatively simple layered Q model for the earth. The modes included 21 ${}_0S_l$, two ${}_0T_l$, and seven ${}_nS_0$ modes, one toroidal overtone, and seven high-Q overtones. They used no body wave data in their analysis. Their preferred model has Q_μ of 110 in the mantle above 670 km and 403 in the lower mantle. In order to satisfy the radial modes they propose a Q_K of 433 in the upper mantle. Their inner core has infinite Q. On the basis of body wave and inner core mode data we prefer a dissipative inner core.

The Sailor and Dziewonski model QBS and model SL8 are compared with the data in Tables 4, 11, and 16. For the spheroidal modes, predicted model Q increase more rapidly from 150 to 300 s for SL8 and more slowly from 700 to 2000 s. The mode data are in agreement with the rapid increase at the shorter periods and cannot discriminate between the models at the longer periods. Decisive measurements of Q for ${}_0S_2$ and ${}_0S_3$ could resolve the differences. For example, the Q for ${}_0S_2$ is predicted to be 540 for SL8 and 576 for QBS. If the high values between 300 and 100 s and the low values for periods beyond 1200 s are supported by future investigations, then the case for an increasing Q with depth in most of the lower mantle and a low-Q zone at the base of the mantle would be strengthened.

Model SL8 was designed to give $t_\alpha^* = 1.0 \pm 0.1$ s between 30° and 90° for shallow focus events. Model QBS gives 1.2–1.4 s over this range; t_β^* is 5.2 ± 0.7 and 3.0 ± 0.5 s for shallow and deep focus events, respectively [*Burdick*, 1977]. SL8 gives 4.6 ± 0.4 and 3.4 ± 0.5 s, and QBS gives 4.8 ± 0.6 and 3.5 ±

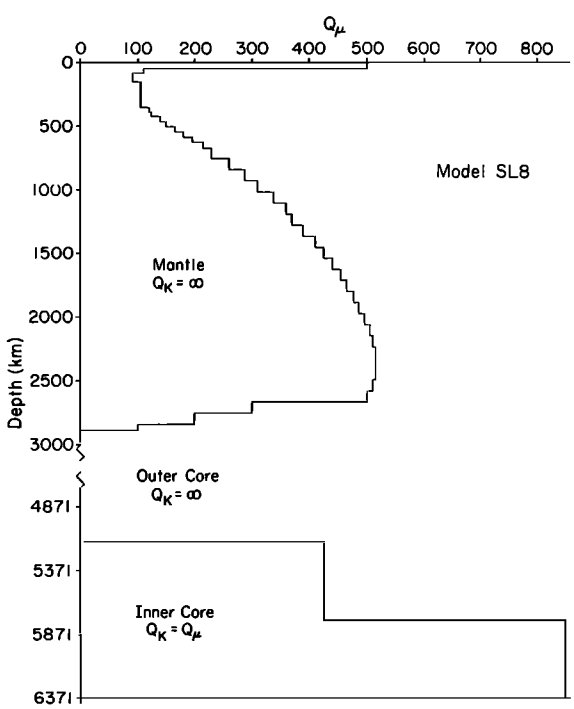

Fig. 6. Q model SL8

TABLE 14. Q Model SL7

Radius, km	Depth, km	Thickness, km	Q_β	Q_α	$1/Q_k$
6371.00	0.0	5.50	500.00	1242.22	0.0
6365.50	5.50	5.50	500.00	1244.11	0.0
6360.00	11.00	34.20	500.00	1047.31	0.0
6325.79	45.20	34.16	110.00	240.20	0.0
6291.62	79.37	34.16	90.00	207.14	0.0
6257.46	113.53	34.16	90.00	218.50	0.0
6223.29	147.70	34.16	105.00	265.92	0.0
6189.13	181.86	34.16	105.00	273.85	0.0
6154.97	216.02	34.16	105.00	279.38	0.0
6120.80	250.19	34.16	105.00	282.06	0.0
6086.64	284.35	34.16	105.00	282.18	0.0
6052.47	318.52	34.16	105.00	280.41	0.0
6018.31	352.68	34.16	105.00	277.89	0.0
5984.15	386.84	34.16	105.00	275.19	0.0
5950.00	421.00	41.68	110.00	285.61	0.0
5908.30	462.69	41.66	200.00	515.20	0.0
5866.64	504.35	41.66	200.00	511.56	0.0
5824.97	546.02	41.66	200.00	507.94	0.0
5783.31	587.68	41.66	200.00	504.18	0.0
5741.65	629.34	41.66	200.00	499.63	0.0
5700.00	671.00	86.06	235.00	578.62	0.0
5613.93	757.07	86.92	280.00	680.00	0.0
5527.00	843.99	86.92	320.00	771.19	0.0
5440.09	930.91	86.92	355.00	852.04	0.0
5353.15	1017.84	86.92	385.00	925.11	0.0
5266.23	1104.76	86.92	385.00	931.93	0.0
5179.31	1191.68	86.92	385.00	941.71	0.0
5092.39	1278.60	86.92	385.00	951.49	0.0
5005.47	1365.52	86.92	385.00	959.93	0.0
4918.54	1452.45	86.92	385.00	967.10	0.0
4831.62	1539.37	86.92	385.00	973.45	0.0
4744.70	1626.29	86.92	385.00	979.08	0.0
4657.78	1713.21	86.92	385.00	983.57	0.0
4570.86	1800.13	86.92	518.00	1326.86	0.0
4483.93	1887.06	86.92	532.00	1362.99	0.0
4397.02	1973.98	86.92	546.00	1397.09	0.0
4310.09	2060.90	86.92	560.00	1432.49	0.0
4223.18	2147.82	86.92	568.00	1456.86	0.0
4136.25	2234.74	86.92	576.00	1486.98	0.0
4049.33	2321.67	86.93	584.00	1522.30	0.0
3962.41	2408.59	86.93	592.00	1560.92	0.0
3875.48	2495.52	86.93	600.00	1599.26	0.0
3788.55	2582.45	86.93	608.00	1633.42	0.0
3701.62	2669.38	86.93	616.00	1661.64	0.0
3614.70	2756.30	86.93	400.00	1079.53	0.0
3527.76	2843.24	43.46	100.00	268.99	0.0
3484.30	2886.70	1157.87	0.00	1,000,000.00	0.100E − 05
2326.40	4044.60	1096.92	0.00	1,000,000.00	0.100E − 05
1229.50	5141.50	614.75	450.00	450.00	0.222E − 02
614.75	5756.25	614.75	900.00	90.00	0.111E − 02

Read 0.100E − 05 as 0.100×10^{-5}.

0.8 s. The average Q_β for the mantle is about the same for both models.

Sailor and Dziewonski [1978] state that models which do not have bulk dissipation in the mantle cannot satisfy the radial mode data. They infer a Q_K of 433 in the upper mantle. SL8 has an average error of 15% for the radial mode data of Sailor and Dziewonski compared to 11% for QBS; both are within the data uncertainties. If the average of published values for the radial modes is used, the errors are 21% for SL8 and 25% for QBS. Comparisons are made in Table 4. Thus we conclude that the radial modes do not require bulk dissipation in the mantle and that they can be satisfied with bulk dissipation in the inner core. This option is also favored by the body wave and inner core mode data.

Two new sets of great circle data have recently become available. *Mills* [1977] and *Nakanishi* [1978] have determined Rayleigh wave attenuation coefficients for 9 and 33 paths, respectively. These data have been combined with previous great circle data to obtain 'global average' Q values (Table 16). The standard deviation in Table 16 refers to the variation of the mean value between individual studies. These obs vations are relevant to the Q structure between 200- and 1000-km depth. The data indicate a rapidly rising Q from 160 to 300 s, in agreement with model SL8. Model QBS predicts a much more slowly increasing Q over this period range. The two models have about the same average Q_μ above 350 km, but SL8 has Q increasing from 350 km to 671 km in the region where QBS has a constant Q. SL8 has a high-Q lithosphere, a low-Q channel in the upper mantle, and no bulk dissipation in the upper mantle. These features, plus the gradient mentioned above, are responsible for the differences between the predictions of the models in Tables 11 and 16.

TABLE 15. Q Model SL8

Radius, km	Depth, km	Thickness, km	Q_β	Q_α	$1/Q_k$
6371.00	0.0	5.50	500.00	1242.22	0.0
6365.50	5.50	5.50	500.00	1244.11	0.0
6360.00	11.00	34.20	500.00	1047.31	0.0
6325.79	45.20	34.16	110.00	240.20	0.0
6291.62	79.37	34.16	90.00	207.14	0.0
6257.46	113.53	34.16	90.00	218.50	0.0
6223.29	147.70	34.16	105.00	265.92	0.0
6189.13	181.86	34.16	105.00	273.85	0.0
6154.97	216.02	34.16	105.00	279.38	0.0
6120.80	250.19	34.16	105.00	282.06	0.0
6086.64	284.35	34.16	105.00	282.18	0.0
6052.47	318.52	34.16	105.00	280.41	0.0
6018.31	352.68	34.16	120.00	317.59	0.0
5984.15	386.84	34.16	124.00	324.98	0.0
5950.00	421.00	41.68	140.00	363.50	0.0
5908.30	462.69	41.66	150.00	386.40	0.0
5866.64	504.35	41.66	166.00	424.59	0.0
5824.97	546.02	41.66	180.00	457.15	0.0
5783.31	587.68	41.66	196.00	494.09	0.0
5741.65	629.34	41.66	215.00	537.10	0.0
5700.00	671.00	86.06	230.00	566.31	0.0
5613.93	757.07	86.92	260.00	631.43	0.0
5527.00	843.99	86.92	287.00	691.66	0.0
5440.09	930.91	86.92	310.00	744.03	0.0
5353.15	1017.84	86.92	338.00	812.18	0.0
5266.23	1104.76	86.92	360.00	871.42	0.0
5179.31	1191.68	86.92	370.00	905.02	0.0
5092.39	1278.60	86.92	390.00	963.85	0.0
5005.47	1365.52	86.92	410.00	1022.26	0.0
4918.54	1452.45	86.92	425.00	1067.57	0.0
4831.62	1539.37	86.92	440.00	1112.51	0.0
4744.70	1626.29	86.92	455.00	1157.09	0.0
4657.78	1713.21	86.92	465.00	1187.94	0.0
4570.86	1800.13	86.92	477.00	1221.83	0.0
4483.93	1887.06	86.92	485.00	1242.57	0.0
4397.02	1973.98	86.92	495.00	1266.60	0.0
4310.09	2060.90	86.92	505.00	1291.80	0.0
4223.18	2147.82	86.92	510.00	1308.10	0.0
4136.25	2234.74	86.92	515.00	1329.50	0.0
4049.33	2321.67	86.93	515.00	1342.44	0.0
3962.41	2408.59	86.93	515.00	1357.89	0.0
3875.48	2495.52	86.93	510.00	1359.37	0.0
3788.55	2582.45	86.93	500.00	1343.27	0.0
3701.62	2669.38	86.93	300.00	809.24	0.0
3614.70	2756.30	86.93	200.00	539.77	0.0
3527.76	2843.24	43.46	100.00	268.99	0.0
3484.30	2886.70	1157.87	0.00	1,000,000.00	$0.100E-05$
2326.40	4044.60	1096.92	0.00	1,000,000.00	$0.100E-05$
1229.50	5141.50	614.75	425.00	425.00	$0.235E-02$
614.75	5756.25	614.75	850.00	850.00	$0.118E-02$

Read $0.100E-05$ as 0.100×10^{-5}.

The lowermost mantle is the most unconstrained part of the earth and therefore the most uncertain feature of the models. This is because body waves penetrating this region are subjected to diffraction effects, excessive scattering and interference. The low Q in this region may not be an intrinsic Q but an apparant value resulting from a combination of the above effects. Nevertheless, it is the appropriate value for many applications. Unfortunately, the scatter of the available low-order spheroidal mode data does not permit a resolution of this problem. All that can be said is that the mode data are consistent with a low-Q zone at the base of the mantle of the nature proposed on the basis of body wave studies.

Summary and Conclusion

Surface wave data for many great circle paths have been used to determine the Q structure of the upper mantle. This structure should represent a good global average. Body wave data are used to estimate the gradient of Q in the lower mantle and the Q in the inner and outer core. Normal mode data, after some reassignments of overtone designations based on excitation calculations, are then checked for consistency with the model. A constraint has been imposed that t^* should be close to values determined from body waves and that it should be relatively constant with distance between 30° and 80°. This leads to a Q that increases smoothly with depth in the lower mantle. The ability to find a model that fits body wave and normal mode data is consistent with, but does not require, a frequency independent Q. This assumption is dropped in a forthcoming paper.

Normal mode and body wave data have been used to argue that there is bulk dissipation, as well as shear dissipation, in the inner core. No bulk dissipation is required in the mantle. Both the body wave and normal mode data suggest that Q increases with depth from 200 to 1000 km.

TABLE 16. Average Values for High-Order Spheroidal Model and Values for Two Models

Mode	T, s	$\bar{Q}$	S.D., %	SL8	QBS	N*
${}_0S_{28}$	297.75	212	11	201	165	81
${}_0S_{29}$	268.54	204	9	180	151	69
${}_0S_{40}$	212.48	170	6	149	134	81
${}_0S_{50}$	178.29	143	6	136	130	72
${}_0S_{51}$	175.44	138	4	135	129	84
${}_0S_{57}$	159.99	128	5	131	129	100
${}_0S_{60}$	153.18	123	4	129	129	56

*Number of great circle paths used in computing average ($\bar{Q}$) and standard deviation (S.D.). Data are from *Deschamps* [1977], *Wu* [1972], *Kanamori* [1970], *Sailor and Dziewonski* [1978], *Nakanishi* [1978], and *Mills* [1977].

Acknowledgments. We thank Hiroo Kanamori, L. Burdick, A. Dziewonski, T. Ahrens, and R. Sailor for their helpful discussions and comments. E. Okal, F. Gilbert, R. Buland, R. Sailor, A. Dziewonski, B. Bolt, D. Brillinger, R. Geller, and S. Stein kindly made available data prior to publication. Freeman Gilbert and Ray Buland provided us with an extensive eigenfunction data tape which was invaluable for the present study. We thank Freeman Gilbert for his recommendations for improving the manuscript. This research was supported by the Advanced Research Projects Agency of the Department of Defense and was monitored by the Air Force Office of Scientific Research under contract F49620-77-0022 and by National Science Foundation grant EAR77-14675. Contribution 2848, Division of Geological and Planetary Sciences, California Institute of Technology, Pasadena, California 91125.

REFERENCES

Adams, R. D., Multiple inner core reflections from a Novaya Zemlya explosion, *Bull. Seismol. Soc. Amer., 62,* 1063, 1972.

Akopyan, S. T., V. N. Zharkov, and V. M. Lyubimora, On the dynamic shear modulus of the earth's interior, *Dokl. Akad. Nauk SSSR, 223,* 1975.

Anderson, D. L., The anelasticity of the mantle, *Geophys. J. Roy. Astron. Soc., 14,* 135–164, 1967.

Anderson, D. L., and C. B. Archambeau, The anelasticity of the earth, *J. Geophys. Res., 69,* 2071–2084, 1964.

Anderson, D. L., and R. S. Hart, An earth model based on free oscillations and body waves, *J. Geophys. Res., 81,* 1461–1475, 1976.

Anderson, D. L., and R. S. Hart, Attenuation models for the earth, *Phys. Earth Planet. Interiors, 16,* 289–305, 1978.

Anderson, D. L., and R. L. Kovach, Attenuation in the mantle and rigidity of the core from multiply reflected core phases, *Proc. Nat. Acad. Sci. U.S., 51,* 168–172, 1978.

Anderson, D. L., A. Ben-Menahem, and C. B. Archambeau, Attenuation of seismic energy in the upper mantle, *J. Geophys. Res., 70,* 1441–1448, 1965.

Anderson, D. L., H. Kanamori, R. S. Hart, and H.-P. Liu, The earth as a seismic absorption band, *Science, 196,* 1104–1106, 1976.

Bhattacharya, B., Excitation and attenuation of Love waves in North America from the November 9, 1968 south central Illinois earthquake, *J. Phys. Earth, 23,* 173–187, 1975.

Ben-Menahem, A., Observed attenuation and Q values of seismic waves in the upper mantle, *J. Geophys. Res., 70,* 4641, 1965.

Berzon, I. S., I. P. Passechnik, and A. M. Polikarpov, The determination of P-wave attenuation values in the earth's mantle, *Geophys. J. Roy. Astron. Soc., 39*(3), 603, 1974.

Bolt, B. A., and D. R. Brillinger, Estimation of uncertainties in fundamental frequencies of decaying geophysical time series (abstract), *Eos Trans. AGU, 56,* 403, 1975.

Buchbinder, G. G., A velocity structure of the earth's core, *Bull. Seismol. Soc. Amer., 61,* 429, 1971.

Buland, R., and F. Gilbert, Improved resolution of complex eigenfrequencies in analytically continued seismic spectra, *Geophys. J. Roy. Astron. Soc., 52*(3), 457, 1978.

Burdick, L., Broad-band seismic studies of body waves, Ph.D. thesis, Calif. Inst. of Technol., Pasadena, 1977.

Carpenter, E. W., Absorption of elastic waves—An operator for a constant Q mechanism, *Rep. 0-43/66,* At. Weapons Res. Estab., London, 1966.

Carpenter, E. W., and E. A. Flinn, Attenuation of teleseismic body waves, *Nature, 207,* 745, 1965.

Cormier, V. F., and P. G. Richards, Comments on 'The damping of core waves' by Anthony Qamar and Alfredo Eisenberg, *J. Geophys. Res., 81,* 3066, 1976.

Davies, D., On the problem of compatibility of surface wave data, Q, and body wave travel times, *Geophys. J. Roy. Astron. Soc., 13,* 421, 1967.

Deschamps, A., Inversion of the attenuation data of free oscillations of the earth (fundamental and first higher modes), *Geophys. J. Roy. Astron. Soc., 50,* 699–722, 1977.

Doornbos, D. J., The anelasticity of the inner cone, *Geophys. J. Roy. Astron. Soc., 38,* 397, 1974.

Douglas, A., J. A. Hudson, P. D. Marshall, and J. B. Young, Earthquakes that look like explosions, *Geophys. J. Roy. Astron. Soc., 36,* 227, 1974.

Dratler, J. W., E. Farrell, B. Block, and F. Gilbert, High Q overtone modes of the earth, *Geophys. J. Roy. Astron. Soc., 23,* 399–410, 1971.

Dziewonski, A., and F. Gilbert, Observations of normal modes from 84 recordings of the Alaskan earthquake of 1964, March 28, *Geophys. J. Roy. Astron. Soc., 27,* 393–446, 1972.

Frazier, C. W., and J. J. Filson, A direct measurement of the earth's short-period attenuation along a teleseismic ray path, *J. Geophys. Res., 77,* 3782, 1972.

Gilbert, F., and A. Dziewonski, An application of normal mode theory to the retrieval of structural parameters and source mechanisms from seismic spectra, *Phil. Trans. Roy. Soc. London, Ser. A, 278,* 187–269, 1975.

Hart, R. S., and R. Butler, Shear wave travel-times and amplitudes for two well-constrained earthquakes, submitted to *Bull. Seismol. Soc. Amer., 68*(4), 973, 1978.

Hart, R. S., D. L. Anderson, and H. Kanamori, Shear velocity and density of an attenuating earth, *Earth Planet. Sci. Lett., 32,* 25–34, 1976.

Hart, R. S., D. L. Anderson, and H. Kanamori, The effect of attenuation on gross earth models, *J. Geophys. Res., 82,* 1647–1654, 1977.

Helmberger, D. V., On the structure of the low velocity zone, *Geophys. J. Roy. Astron. Soc., 34,* 251, 1973.

Helmberger, D. V., and G. R. Engen, Upper mantle shear structure, *J. Geophys. Res., 79,* 4017, 1974.

Jeffreys, H., The damping of S waves, *Nature, 208,* 675, 1965.

Jobert, N., and G. Roult, Periods and damping of free oscillations observed in France after sixteen earthquakes, *Geophys. J. Roy. Astron. Soc., 45,* 155–176, 1976.

Jordan, T. H., and D. L. Anderson, Earth structure from free oscillations and travel-times, *Geophys. J. Roy. Astron. Soc., 36,* 411, 1974.

Julian, B. R., D. Davies, and R. M. Sheppard, *PKJKP, Nature, 235,* 317, 1972.

Kanamori, H., Spectrum of P and PcP in relation to the mantle-core boundary and attenuation in the mantle, *J. Geophys. Res., 72,* 559, 1967*a*.

Kanamori, H., Attenuation of P waves in the upper and lower mantle, *Bull. Earthquake Res. Inst. Tokyo Univ., 45,* 299, 1967*b*.

Kanamori, H., Spectrum of short-period core phases in relation to the attenuation in the mantle, *J. Geophys. Res., 72,* 2181, 1967*c*.

Kanamori, H., Velocity and Q of mantle waves, *Phys. Earth Planet. Interiors, 2,* 259–275, 1970.

Kanamori, H., and D. L. Anderson, Importance of physical dispersion in surface-wave and free-oscillation problems: Review, *Rev. Geophys. Space Phys., 15,* 105–112, 1977.

Kovach, R. L., and D. L. Anderson, Attenuation of shear waves in the upper and lower mantle, *Bull. Seismol. Soc. Amer., 54,* 1855–1864, 1964.

Kuster, G. T., Seismic wave propagation in two-phase media and its applications to the earth's interior, Ph.D. thesis, Mass. Inst. of Technol., Cambridge, 1972.

Liu, H.-P., D. L. Anderson, and H. Kanamori, Velocity dispersion due to anelasticity: Implications for seismology and mantle composition, *Geophys. J. Roy. Astron. Soc., 47,* 41, 1976.

Mikumo, T., and T. Kurita, Q distribution for long-period P waves in the mantle, *J. Phys. Earth, 16,* 11. 1968.

Mills, J. M., Jr., Rayleigh wave group velocities and attenuation coefficients, Ph.D. thesis, 267 pp., Aust. Nat. Univ. Canberra, 1977.

Mitchell, B. J., Surface wave attenuation and crustal anelasticity in central North America, *Bull. Seismol. Soc. Amer., 63,* 1057–1071, 1973.

Mitchell, B. J., and D. V. Helmberger, Shear velocities at the base of the mantle from observations of *S* and *ScS*, *J. Geophys. Res., 78,* 6009, 1973.

Muller, G., Amplitude studies of core phases, *J. Geophys. Res., 78,* 3469, 1973.

Nakanishi, I., Phase velocity and Q of mantle Rayleigh waves, *Geophys. J. Roy. Astron. Soc.,* in press, 1978.

Ness, N. F., J. C. Harrison, and L. B. Slichter, Observations of the free oscillations of the earth, *J. Geophys. Res., 66,* 621–629, 1961.

Nowroozi, A. A., Measurement of Q values from the free oscillations of the earth, *J. Geophys. Res., 73,* 1407–1415, 1968.

Nowroozi, A. A., Characteristic periods and Q for oscillations of the earth following an intermediate-focus earthquake, *J. Phys. Earth, 22,* 1–23, 1974.

Otsuka, M., On the forms of the *S* and *ScS* waves of some deep earthquakes (in Japanese), *Jisin, 15*(2), 169, 1962.

Press, F., Seismic wave attenuation in the crust, *J. Geophys. Res., 69,* 4417–4418, 1964.

Qamar, A., and A. Eisenberg, The damping of core waves, *J. Geophys. Res., 79,* 758, 1974.

Randall, M. J., Attenuative dispersion and frequency shifts of the earth's free oscillations, *Phys. Earth Planet. Interiors, 12,* 1, 1976.

Roult, G., Attenuation of seismic waves of very low frequency, *Phys. Earth Planet. Interiors, 10,* 159–166, 1975.

Sacks, I. S., Anelasticity of the outer core, Annual Report of the Director, Department of Terrestrial Magnetism, 1969–1970, 414 pp., Carnegie Institution, Washington, D. C., 1971*a*.

Sacks, I. S., Anelasticity of inner core, Annual Report of the Director, Department of Terrestrial Magnetism, 1969–1970, 416 pp., Carnegie Institution, Washington, D. C., 1971*b*.

Sacks, I. S., Q structure of the inner and outer core (abstract), *Eos Trans. AGU, 53,* 601, 1972.

Sacks, I. S., and J. A. Snoke, Heterogeneous structure at the base of the mantle, 2, Observations and interpretations, paper presented at the 11th International Symposium on Mathematical Geophysics, Int. Union of Geol. and Geophys., Seeheim, West Germany, 1976.

Sailor, R. V., and A. Dziewonski, Attenuation of a shear energy in the mantle from normal mode analysis, Semi-Annual Technical Report on Seismic Discrimination, pp. 23–25, Lincoln Lab., Cambridge, Mass., 1975.

Sailor, R. V., and A. M. Dziewonski, Measurements and interpretation of normal mode attenuation, *Geophys. J. Roy. Astron. Soc., 53,* 559–581, 1978.

Slichter, L. B., Spherical oscillations of the earth, *Geophys. J. Roy. Astron. Soc., 14,* 171–177, 1967.

Smith, S. W., An investigation of the earth's free oscillations, Ph.D. thesis, Calif. Inst. of Technol., Pasadena, 1961.

Smith, S. W., The anelasticity of the mantle, *Tectonophysics, 13,* 601–622, 1972.

Stein, S., and R. J. Geller, Attenuation measurements of split normal modes for the 1960 Chilean and 1964 Alaskan earthquakes, *Bull. Seismol. Soc. Amer.,* in press, 1978.

Steinhart, H. S., T. J. Smith, I. S. Sacks, R. Sumner, Z. Suzuki, A. Rodriguez, C. Lomnitz, M. A. Tuve, and L. T. Aldrich, Explosion seismology, *Carnegie Inst. Wash. Yearb., 62,* 286, 1964.

Teng, T. L., Attenuation of body waves and the Q structure of the mantle, *J. Geophys. Res., 73,* 2195, 1968.

Tsai, Y. B., and K. Aki, Simultaneous determination of the seismic moment and attenuation of seismic surface waves, *Bull. Seismol. Soc. Amer., 59,* 275–288, 1969.

Wu, F. T., Mantle Rayleigh wave dispersion and tectonic provinces, *J. Geophys. Res., 77,* 6445–6453, 1972.

Yoshida, M., and M. Tsujiura, Spectrum and attenuation of multiply reflected core phases, *J. Phys. Earth, 23,* 31, 1975.

(Received February 2, 1977;
revised August 16, 1978;
accepted September 18, 1978.)